

Using short-range signals from continuous wave excitation to develop a geo-acoustic model of a shallow-water seabed

Marshall V. Hall

Midspar Systems Pty Ltd, Oyster Bay NSW 2225 Australia
(present address: 9 Moya Crescent, Kingsgrove NSW 2208 Australia)

ABSTRACT

Propagation runs, during which a hydrophone was successively placed at ranges from 19 m out to 68 m from a projector, have been conducted in seawater 12 m deep. Tones were emitted at frequencies of 200, 400 and 800 Hz. An inversion has been conducted on the received SPL for the purpose of obtaining a simple Geo-Acoustic Model (GAM) that gives an optimum fit to the data. The GAM was assumed to comprise two homogeneous layers overlying a homogeneous basement. Five parameters were nominated as unknowns for the inversion: porosities of the two layers and of the basement, and thicknesses of the two layers. In computing the cost function, the data from the three runs were included simultaneously, so that one GAM would be obtained that would be optimum for the frequency band from 200 to 800 Hz. For each porosity tried during the inversion, the acoustic properties of the layers and basement were calculated using published regressions; the second layer and basement were treated successively as uncemented and cemented sediment. Consequent Transmission Losses were calculated using the “Ocean Acoustic and Seismic Transmission” (OAST) mathematical model. The best agreement with acoustic data was obtained with the second layer uncemented and the basement cemented, but the best agreement with nearby geological data was obtained with both the layer and basement cemented. The former yielded optimum layer thicknesses of 0.76 and 1.07 m, while the latter yielded 1.48 and 6.85 m. The latter also yielded porosities compatible with the geological data, which indicated a 4-m layer of loose silty sand overlying a layer of medium sand limestone and dense sand.

INTRODUCTION

Particular areas in the sea, known as “sound ranges”, are selected for calibrating hydrophones, measuring noise radiated by underwater vehicles, or the target strengths of such vehicles. Where possible, sound ranges are placed in deep water, so as to reduce the influence of reflections from the seafloor. If a shallow water area is selected then, even though the geological properties of seabed are measured, it is generally acknowledged that such measurements do not characterise the acoustic properties of the seabed with sufficient accuracy. Instead, direct acoustic measurements are required. Although it is possible to directly measure the reflectivity of the seafloor in deep water, it is difficult in shallow water, since the nearby sea surface dominates the total field. An alternative approach is to measure Transmission Loss (TL) as a function of range across the sound range, and from this data use geo-acoustic inversion to produce a Geo-Acoustic Model (GAM) of the seabed. These measurements should be repeated at a number of frequencies that span and sample the frequency band of interest. During the inversion, TL is computed at a large number of realisations of the GAM, and compared with the data. This approach has been followed for one particular sound range, and the results from a preliminary measurement are the subject of this paper. The TL algorithm selected was “Ocean Acoustic and Seismic Transmission” (OAST), written by Schmidt (1999).

THE MEASUREMENTS

The acoustic data used for this paper were obtained with the following procedure.

1. A J11 sound projector was suspended from a horizontally fixed pontoon at a depth of 2.00 m

2. At each of around 24 discrete ranges between the minimum range (19 m) and the maximum range (67 m) from the projector, the hydrophone buoy was held stationary for around 30 s.
3. During each such period, a ping 20-s in duration was emitted by the projector. The frequency remained fixed for the duration of each run.

Various acoustic runs were conducted, and frequencies from 200 Hz to 6300 Hz were encompassed. For the present inversion, the runs that used frequencies of 200, 400 and 800 Hz were selected. Details of these runs are listed in Table 1. The tide heights were estimated from tidal data listed in Table 2. For each run, the hydrophone was suspended from a marker buoy that was towed along the propagation path, and stabilised when stationary, with ropes to both ends of the path. When stationary, the hydrophone depth was measured as 2.17 m.

Table 1: Details of the three acoustic runs.

Measurement	Run 801	Run 825	Run 850
Time (on 8 May 2008)	10:09-10:35	10:57-11:24	11:26-11:58
Frequency (Hz)	200	400	800
Number of stationary positions	24	25	25
Estimated tide height (m)	1.28	1.28	1.26

Ranges from the projector to the buoy were measured with a laser rangefinder, with an accuracy of approximately 0.5 metre.

In addition to the acoustic experiments, the bathymetry along the propagation path was measured, and temperature profiles were obtained at each end of the propagation path. High and low tide heights were noted from a standard web-based tidal model (Bureau of Meteorology, 2009). A chronology of these measurements is listed in Table 2.

Table 2: Details of the environmental measurements

Measurement	High tide	Bathymetry	Temperature profiles	Low tide
Time (on 8 May 2008)	10:33	Approx 13:00	13:53-13:58	21:33
Estimated tide height (m)	1.28	1.20	1.13	0.49

When the seafloor depth was measured along the propagation path, the result was an average of 11.5 m with a standard deviation of 0.09 m. Since the tide heights during the acoustic runs were only 6 to 8 cm (0.5% to 0.7%) greater than during the bathymetry run, the seafloor depths for these runs were maintained at 11.5 m.

The results for water temperature are summarised in Table 3. The corresponding sound-speeds were computed assuming a salinity of 35 ppt.

Table 3: Results for water temperature and the estimated sound-speeds .

Position	Depth (m)	Temperature (°C)	Sound-speed (m/s)
Projector	0	20.6	1523.3
	~ 0.05	20.4	1522.6
	10	19.7	1520.7
Far end of propagation path (range 78 m)	0	20.4	1522.6
	10	19.7	1520.7

Subsequent analysis of the recorded acoustic data began with filtering in appropriate frequency bands. The filter bandwidth was varied between 1% and 4% of the centre frequency, but was held fixed during any particular run. The second stage was to note the average (uncalibrated) intensity of the filtered signal over particular time intervals. Each resulting signal intensity was converted to Signal Loss, which was then presented as a function of range. The results for the three runs are shown in Figure 1.

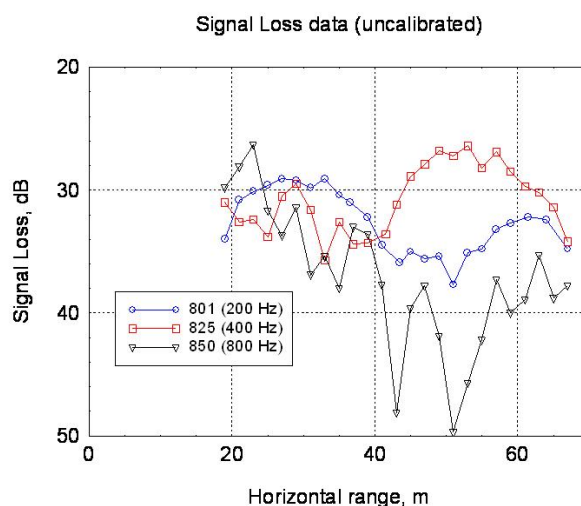


Figure 1: The uncalibrated Signal Losses measured during the three runs, as functions of range

PARAMETERS TO BE OBTAINED BY INVERSION OF THE DATA

Before inverting Signal Loss data in order to obtain an optimum GAM, an issue to address is the appropriate number of parameters to be treated as unknowns. This number is related to the number of orthogonal functions that would be required to fit the data (as functions of range, in the case of the present experiments). For example, if one were to fit polynomial functions of range to the data, how many terms would be required, and could thus be obtained, from that process? In the case of 200 Hz, a polynomial of order 4 fits the data (when converted from dB to “linear” intensity) with small error. For 400 Hz, a polynomial of order 7 fits the data (with some error), while for 800 Hz a polynomial of order 8 replicates most of the range-dependence.

If one uses a number of unknowns that is too high, then a GAM that yields a good fit will be obtained, but in addition there will be a number of alternative GAMs that will also yield good fits. Whether one GAM is superior to another may depend on small changes (within experimental error) in a small number of data points, and thus be of no significance. It is therefore important to select a number of unknowns that will be robustly sustained by the available data.

TL algorithms require that the GAM consist of a number of layers (L) overlying a basement. The layers are characterised by their thicknesses and acoustic properties (of which there are five, to be described in the next section), while the basement is characterised by its acoustic properties. If the acoustic properties in each layer are treated as independent rather than linked, then the number of unknowns (N) is $N = 6L + 5$. For $L = 0, 1,$ and $2, N = 5, 11,$ and 17 respectively.

For any stratum (layer or basement) that is solid (has a non-zero shear-speed), OAST requires that stratum to be uniform with depth. Low values of L (0 or 1) are therefore unlikely to replicate profiles that are found in nature. If one considers $L = 2$, it seems likely that the data (Figure 1) may not sustain an inversion with 17 unknowns (such an inversion operation was conducted, but it yielded unphysical results for some of the properties). Since a realistic GAM with (17) independent properties cannot be obtained, the aim of the present work is to determine whether a useful GAM can be obtained with a small number of unknowns. This is done by linking the acoustic properties to a single parameter (porosity), and thus reducing the number of unknowns to $2L + 1$. This procedure is also likely to prevent any properties from ending up with unphysical values

RELATIONSHIPS BETWEEN ACOUSTIC PROPERTIES AND POROSITY

In order to compute TL along a path over a given seabed, the first step is to divide the seabed into appropriate layers and a basement. The second step is to prescribe the thicknesses of the layers, together with the acoustic properties of the layers and the basement. These acoustic properties are: bulk density, sound and shear speeds, and sound and shear absorption coefficients. Sediment grains can be either cemented or uncemented, and in the present analysis both possibilities are considered.

Density

Bulk density (D_y) is obtained using the following (exact) expression:

$$D_y = p D_w + (1 - p) D_g,$$

where p is porosity, D_w is water density (approximately 1025 kg/m^3), and D_g is the density of solid grain (at zero porosity). For pure calcite and quartz, the constituents of the sediments at the test site, D_g would be 2710 and 2650 kg/m^3 respectively. Since no quantitative data are available for the relative amounts of these constituents in the seabed being studied, they are assumed to be present in equal parts by volume, and the resulting estimate of D_g is 2680 kg/m^3 .

Sound speed

For un-cemented sediment the regression used is that obtained by Richardson and Briggs (2004) for "all sediments". This regression yields the ratio C_p / C_w as a quadratic function of porosity, where C_p and C_w are the sound-speeds in the seafloor and adjacent water respectively. Richardson and Briggs also presented a regression for calcareous sediment in particular, but this was ignored since it produces unrealistic low values for C_p / C_w (~ 0.7) at high porosity.

For cemented sediment, the regressions obtained by Hamilton (1978) in terms of density (for chalk and limestone) are used.

Shear speed

For un-cemented sediment the regression derived by Bryan and Stoll (1988) for shear modulus is employed. This regression is a decreasing function of porosity, and an increasing function of confining pressure, the latter being an increasing function of depth beneath the seafloor. In unconsolidated sediment (porosity at least 0.35), shear speed (C_s) is approximately zero at the seafloor and increases significantly with depth. In view of this depth dependence, the value of C_s at the mid-depth of each layer is used, due to the above-mentioned requirement of OAST that layers of solid be homogeneous. For a basement, a depth of 2 m below the interface was selected, since using this depth yielded good agreement in an example where TL was computed with a shear-speed depth profile (Jensen, 1991), and compared with TLs computed using various depth-independent values for C_s .

For cemented sediment, the recommendation by Hamilton (1980) that C_s be set to $C_p / 1.9$ is adopted

Sound absorption

The regression derived by Hamilton (1972) in terms of porosity has been used, but modified for porosities less than 0.467 (Hamilton's first break-point). The unit of Hamilton's coefficient, which he denoted by K_p , is dB / m / kHz . The minimum porosity in Hamilton's plot is 0.36, and much of the data in the interval $0.36 < p < 0.467$ lie below his linear regression.

Extrapolating the trend of the data to zero porosity indicates that the limits of both K_p and its derivative are likely to be approximately zero as $p \rightarrow 0$. For $0 < p < 0.467$, K_p has therefore been defined by $K_p = 0.521 (p / 0.467)^2$, which approaches Hamilton's value of 0.521 as $p \rightarrow 0.467$. Once computed, K_p is multiplied by $C_p / 1000$ to convert to "Ap" in dB / wavelength , the coefficient required by OAST.

Shear absorption

The shear absorption coefficient ("As" dB / wavelength) is computed as a multiple of the sound absorption, the multiple being an in-house quadratic function of the ratio C_s / C_p , such that the result is consistent with the majority of the data for these four parameters presented by Vasilev and Gurevich (1962). For any layer, if C_s is small, then A_s will have little effect on the computed TL, even though A_s far exceeds A_p .

Interface roughness

Roughness is potentially a relevant parameter, but has not been included in the present study. In view of the short range and low frequencies (large wavelengths), the effect of any feasible roughness on the measured signals is expected to be negligible.

PRELIMINARY OPERATIONS

Before commencing the inversion with a layered seabed, two preliminary operations were conducted with a view to obtaining an estimate of the GAM. In the first, the seabed was assumed to be a uniform basement only, and characterised by its porosity. At each frequency, the correlation (R) between the Signal Loss data and the computed TL was obtained as a function of porosity, and converted to a "Cost" given by $1 - R$. The results are shown in Figure 2. At 800, 400 and 200 Hz, the optimum porosities are 0.66, 0.42, and 0.80 respectively. Since the higher frequencies will be more affected by the upper seabed, it is reasonable to expect that the porosity averaged over a top layer (of unknown thickness) will be around 0.66, and that the porosity averaged over a thicker layer will be around 0.42. From the 200-Hz result, the initial estimate of the average porosity over a great depth interval would be high (around 0.8), which represents a change in the trend noticed from 800 Hz to 400 Hz. The significance of this estimate is tempered by the fact that at 200 Hz, the cost function is a slowly varying function of porosity.

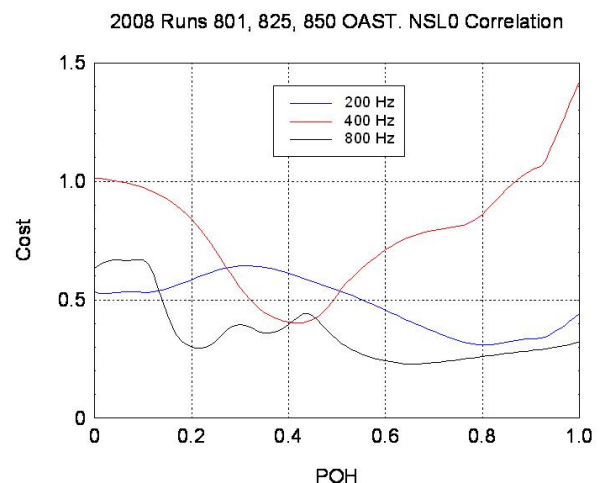


Figure 2: The cost functions ($1 - \text{Correlation Coefficient}$) at three separate frequencies, as functions of the porosity of a hypothetical homogeneous (non-layered) seabed.

In the second preliminary operation, the seabed was assumed to contain one layer, the porosities of the layer and basement were assumed to be 0.66 and 0.42 respectively, and the cost function was computed as a function of layer thickness, for the three frequencies simultaneously. The result is shown in Figure 3. It is evident that the minimum cost occurs at a thickness of 1.2 m.

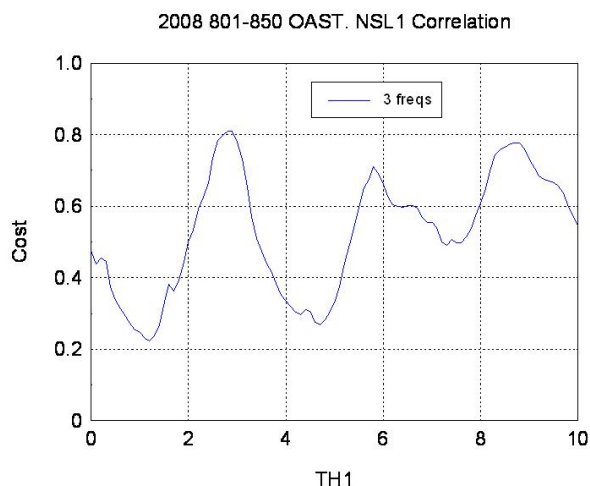


Figure 3: Cost function (1 – R) for a seabed with one layer, as a function of layer thickness. The porosities of the layer and basement are those identified in Figure 2 as optimum porosities at 800 and 400 Hz respectively. The cost function is averaged over the three frequencies.

MAIN INVERSION OPERATIONS

For the main inversion, the data at frequencies 200, 400 and 800 Hz were included together, so that the GAM obtained that would be the optimum for the frequency band encompassed by these runs. The overall cost at each GAM is the average of the costs of the three runs.

A seafloor depth of 11.5 m was used for the computation of TL.

To date, 19 inversion operations have been conducted, to evaluate the results obtained with various numbers of layers, and various sets of unknown parameters. The Simulated Annealing algorithm due to Goffe et al (1994) was used. A sequence of “temperatures” (that decrease by a fixed proportion) was defined, and input parameters were set such that the cost function was evaluated 125 times at each temperature. The initial temperature was set to 0.05 during the first 15 operations, and 0.1 subsequently. The latter is somewhat greater than the standard deviation of the cost function when evaluated over a range of porosities and thicknesses. To start, the Simulated Annealing algorithm randomly chooses a trial point within the step length (a vector with one component for each unknown parameter) of the user-selected starting point. For each parameter the initial step length is the difference between the user-defined lower and upper bounds. During each temperature stage, each step length component is periodically adjusted so that half of all function evaluations at different values of that parameter are accepted. Input parameters that affect termination of an operation were set such that if the final cost function values from the last three temperatures differ from the corresponding value at the current temperature by less than 10^{-4} , the operation will terminate.

Three operations have been selected for presentation in the present paper. They all assume that $L = 2$, that each layer is characterised by two parameters (thickness and porosity), and that the basement is characterised by one parameter (porosity).

The differences amongst these operations related to assumptions about whether each stratum was cemented or un-cemented sediment:

- the two layers and basement were all assumed to be un-cemented (Operation 9). This configuration is denoted by ‘UUU’.
- the first layer was un-cemented, and the second layer and basement were cemented (Operation 18). This configuration is denoted by ‘UCC’.
- the two layers were un-cemented, and the basement cemented (Operation 19). This configuration is denoted by ‘UUC’.

The lower and upper bounds for the five unknown parameters are listed in Table 4. The bounds for the porosities were guided by the results obtained in the first preliminary operation. Some of the values are somewhat arbitrary, but are displayed as a matter of record. A modification to the Simulated Annealing algorithm (introduced by the present writer) allows each unknown to escape from its bounds, once the temperature number reaches a pre-defined value, set to 9 for the present study. (From around that stage, there should be no need to maintain an arbitrary constraint, since appropriate step lengths will have been computed for the unknowns.)

Table 4: Initial lower and upper bounds for the five inversion parameters.

Operation	Unknown:	TH1	PO1	TH2	PO2	POH
9	Lower bound:	0	0.5	0	0.3	0.2
(UUU)	Upper bound:	5	0.8	5	0.5	0.3
18	Lower bound:	0	0.6	0	0.4	0.2
(UCC)	Upper bound:	10	0.8	10	0.6	0.4
19	Lower bound:	0	0.6	0	0.4	0.2
(UUC)	Upper bound:	10	0.8	10	0.6	0.4

The history of the cost function during Operation 9, which terminated after 23 temperatures (2875 function evaluations), is shown in Figure 4. The histories during the other two operations are similar; except that they took longer to terminate (Operations 18 and 19 terminated after 24 and 27 temperatures respectively). The parameter RT shown in the figure heading is the ratio of each temperature to its predecessor. The parameter NT is the number of times at each temperature that the step length is adjusted (the cost function was evaluated 25 times at each step length).

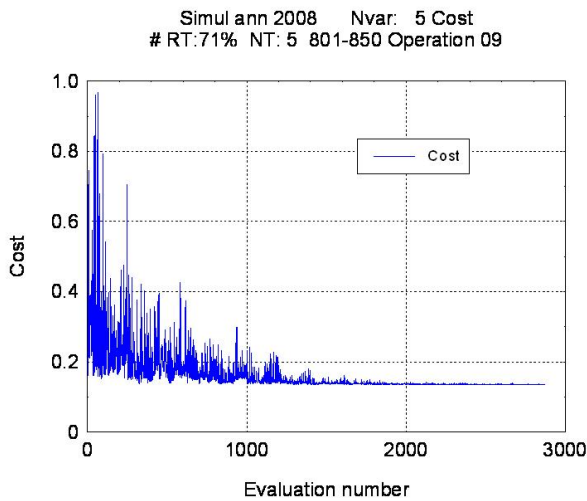


Figure 4: History of the cost function during Operation 9 (UUU).

The histories of the two layer thicknesses during Operation 9 are shown in Figure 5. The histories for Operation 19 are similar, but for Operation 18 the value that TH2 converges to is 6.85 m, several times larger than its values for operations 9 and 19.

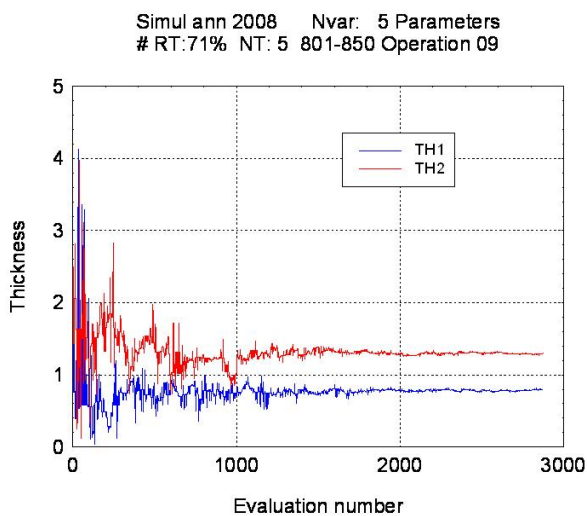


Figure 5: Histories of the two layer thicknesses during Operation 9 (UUU).

The histories of the three porosities (two layers and basement) during operation 9 are shown in Figure 6. Operation 18 yields porosities similar to Operation 9, while Operation 19 yielded significantly higher porosities.

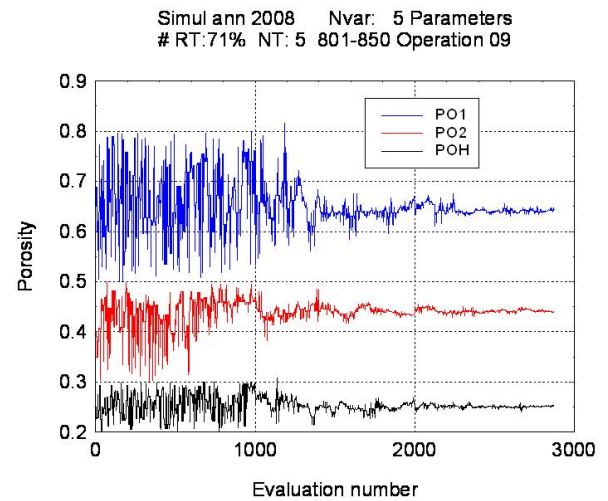


Figure 6: Histories of the three porosities during Operation 9 (UUU).

For each of the three operations, the optimum values of the five parameters are listed in Table 5.

Table 5: Optimum values for the five inversion parameters.

Operation	Cementation	TH1	PO1	TH2	PO2	POH
9	UUU	0.79	0.64	1.29	0.44	0.25
18	UCC	1.48	0.64	6.85	0.48	0.18
19	UUC	0.76	0.87	1.07	0.63	0.40

The optimum costs (averaged over the three frequencies) for these three operations were 0.136, 0.152, and 0.095 respectively. These correspond to correlations of 0.864, 0.848 and 0.905.

These results can be examined for their internal consistency, since low porosity sediments are likely to be cemented, while high porosity sediments are likely to be un-cemented. For Operation 9, the results for the layers are self-consistent, but a basement with porosity 0.25 is more likely to be cemented. For Operation 18, the results for layer 1 and the basement are self-consistent, but layer 2 with porosity 0.48 is more likely to be un-cemented. For Operation 19, the results for the layers are self-consistent, but a basement with porosity 0.40 is more likely to be un-cemented.

For a bottom water sound speed (C_w) of 1520.7 m/s, the corresponding GAM obtained from Operation 9, using the regressions listed above, is listed in Table 6. Each acoustic property is displayed with four numerals, although the average number of significant figures would be three.

Table 6: The GAM that corresponds to the optimum porosity profile from Operation 9 (UUU), and a seawater sound-speed of 1520.7 m/s

Depth below seafloor (m)	C_p (m/s)	C_s (m/s)	A_p (dB / wave-length)	A_s (dB / wave-length)	D_y (kg/m^3)
0	1527	44.55	0.270	2.189	1621
0.79	1679	119.9	0.779	5.617	1950
2.08	1935	212.2	0.291	1.872	2265

PERFORMANCE OF THE OPTIMUM GAM

Using the optimum GAMs, TL has been computed at the measurement frequencies, smoothed in accordance with the analysis bandwidth and averaging times, and overlaid on graphs of the measured data. The results for the 200-Hz run are shown in Figure 7. The green curve is the uncalibrated “Signal Loss” of the acoustic signal measured at 25 discrete ranges. The blue, red and black curves are TL computed with OAST using the inversion GAMs from Operations 9, 18, and 19. These have been computed at the 25 measurement ranges and corrected for bandwidth and averaging time. The important aspect is not the arbitrary offset (of a few dB) between the curves, but the high correlations between the points in the green curve with those in the other curves. Since the costs (1-R) are 0.10, 0.10, and 0.14 respectively, Operations 9 and 18 yielded equal best agreement with the data.

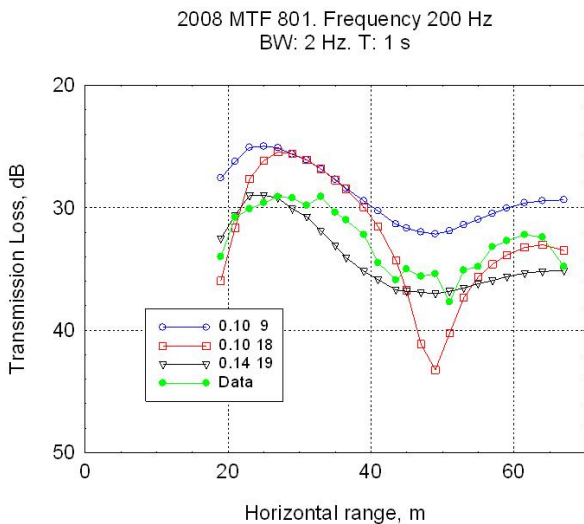


Figure 7: Transmission Losses at 200 Hz. Key: green – measured uncalibrated data; blue, red & black – computed with OAST using the optimum GAMs from Operations 9, 18 & 19.

The results for 400 Hz are shown in Figure 8. Since the costs for the three operations at this frequency are 0.18, 0.18, and 0.08, Operation 19 yielded the best agreement with the data at this frequency.

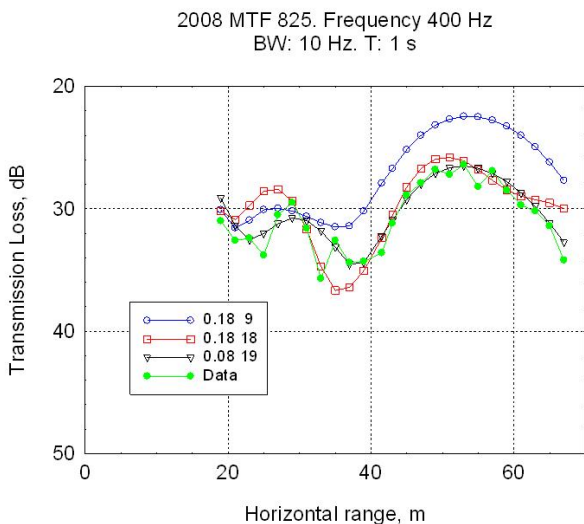


Figure 8: Transmission Losses at 400 Hz. Key: as for Figure 7.

The results for 800 Hz are shown in Figure 9. The costs for the three operations at this frequency are 0.13, 0.17, and 0.07,

and thus Operation 19 yielded the best agreement with the data at this frequency also.

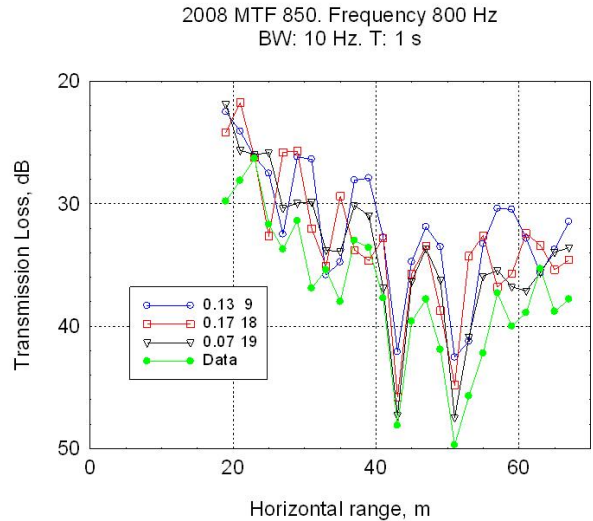


Figure 9: Transmission Losses at 800 Hz. Key: as for Figure 7.

COMPARISON WITH GEOLOGICAL DATA

Pre-existing geological data closest to the propagation path were obtained from a borehole located around 70 m to the side of the path. These data had been collected with the aim of describing the geotechnical properties of the seabed (for sustaining a jetty). The seafloor depth at this borehole was 8.7 m, some 3 m shallower than along the propagation path. The descriptions provided of the first three layers (of a total of five) were as follows:

First layer (4 m thick): “loose grey-black, silty, medium grained sand with some calcareous nodules”. Near the middle of this layer, the “Standard Penetration Resistance” was given an N value of 9, indicating loose sand. The N parameter is the number of blows by a standard hammer needed to drive a standard penetrometer a further 30 cm from a depth 15 cm beneath the soil surface, in this case the bottom of a borehole (Craig 2004). The density (denoted by “gamma”) at the bottom of this layer was given as 1630 kg/m³.

Second layer (2 m thick): “hard, grey, medium grained quartz sand limestone, and dense grey sand & shells 6’ to 10’ sticks”. Near the top and bottom of this layer, the N values were 300 and 600 respectively, indicating very dense sand.

Third layer (6 m thick): “hard, yellow-white, coarse grained quartz sand limestone with some dense coarse grained sand”. From the top to the bottom of this layer, the N values increased from 300 to 600, again indicating very dense sand. Densities near the top, middle and bottom of this layer were given as 1810, 1950, and 2100 kg/m³ respectively. The corresponding porosities (assuming D_g = 2680 kg/m³) are 0.53, 0.44, and 0.35 respectively. It seems surprising that a sand that seems “very dense” to a penetrometer would have a porosity of 0.53.

A comparison of the inversion and geological porosity profiles is shown in Figure 10. It can be seen that Operation 18 (UCC) yielded the best agreement with the geological profile. The porosities are similar, and their gradients (if smoothed) would be somewhat similar. For Operations 9 and 19 the porosity ranges are compatible, but there is a large difference in the rate of change in porosity with depth. On this basis, it

appears that the UCC operation yielded the most realistic profile.

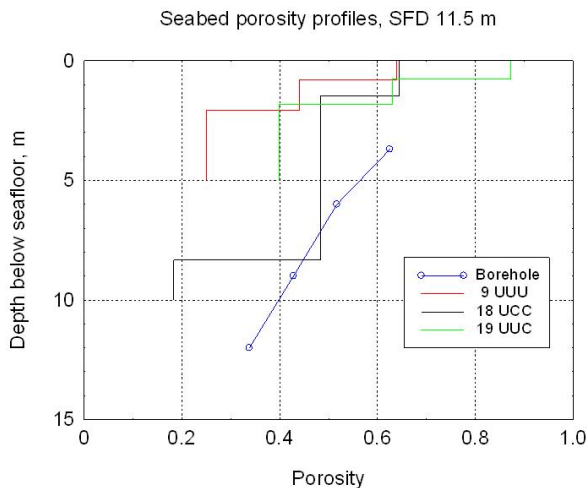


Figure 10. Comparison of the geotechnical and the three inversion porosity profiles. The borehole was around 70 m to the side of the acoustic propagation path.

CONCLUSIONS AND REMARKS

Geo-acoustic inversion operations with five unknown parameters have been applied to acoustic data spanning two octaves. The operations made different assumptions about whether the seabed strata were cemented or not. The operation that assumed the first layer to be un-cemented and the second layer and basement to be cemented yielded satisfactory agreement with a profile obtained geo-technically some 70 m away. Operations that made other assumptions about cementation of the strata yielded unsatisfactory agreement. The inversion result shows some internal inconsistency, in that a layer postulated to be cemented had an uncharacteristically high porosity (0.48). This may indicate that this layer contained a mixture of cemented and un-cemented sediment, rather than entirely one or the other.

An aspect that needs to be kept in mind when subsequently applying the GAM is that, since the layers are saturated with seawater, their sound speeds will vary with seasonal variations in C_w ; since the constant parameter is the ratio C_p / C_w , rather than C_p .

ACKNOWLEDGMENT

The Defence Science and Technology Organisation - Stirling (Garden Island, Western Australia) provided the data, funded the analysis, and gave permission for this paper to be published.

The two anonymous referees made useful comments.

REFERENCES

Bryan G. M. And Stoll R. D. 1988, "The dynamic shear modulus of marine sediments", *Journal of the Acoustical Society of America*, vol. 83, pp 2159-2164.

Bureau of Meteorology 2009, <http://www.bom.gov.au/oceanography/tides/MAPS/wa.shtml#map>

Craig, R. F. 2004, *Craig's soil mechanics*, Taylor & Francis, London UK (online).

Goffe, W.L., Ferrier, G.D. & Rogers, J. 1994, "Global optimization of statistical functions with simulated annealing", *Journal of Econometrics* vol. 60, pp 65 – 99.

Hamilton, E. L. 1972, "Compressional wave attenuation in marine sediments", *Geophysics*, vol. 37, pp 620-645.

Hamilton, E. L. 1978, "Sound velocity-density relations in sea-floor sediments and rocks", *Journal of the Acoustical Society of America*, vol. 63, pp 366-377.

Hamilton, E. L. 1980, "Geoacoustic modeling of the sea-floor", *Journal of the Acoustical Society of America*, vol. 68, pp 1313-1340.

Jensen, F. B. 1991, "Excess attenuation in low-frequency shallow-water acoustics: a shear wave effect?", in: J. M. Hovem et al (eds.), *Shear waves in marine sediments*, Kluwer Academic Publishers, The Netherlands, pp 421-430.

Richardson, M. D. and Briggs, K. B. 2004, "Relationships among sediment physical and acoustic properties in siliciclastic and calcareous sediments", *Proceedings of the Seventh European Conference on Underwater Acoustics, ECUA 2004*, Delft, The Netherlands.

Schmidt, H. (1999) *OASES Ocean Acoustics and Seismic Exploration Synthesis* (version 2.2). Retrieved 1999, from <http://acoustics.mit.edu/faculty/henrik/oases.html>

Vasilev, Y. I. and Gurevich, G. I. 1962, "On the ratio between attenuation decrements and propagation velocities of longitudinal and traverse waves", *Bulletin of the USSR Academy of Sciences, Ser. Geophys.* No. 12, pp 1061-1074. [English Translation].